



GIS HYDROLOGICAL MODELS FOR MANAGING WATER RESOURCES IN THE INDIAN YERRAKALAVA RIVER BASIN: A CASE STUDY

ANDE R.^{1}, CHADEE A.A.², MANAS D.^{3*}, VERMA S.⁴, THAKUR S.S.⁵*

^{1*} Department of Fabric and Apparel Science, Lady Irwin College, University of Delhi,
New Delhi, 110001, India

² Lecturer, Department of Civil and Environmental Engineering, University of the West
Indies, Saint Augustine Campus, Trinidad and Tobago RY1HKEY93NN6.

^{3*} Assistant Professor, Civil Engineering Department, Shri Shankaracharya Institute of
Professional Management and Technology Raipur (C.G.), 492015, India

⁴ Project Scientist, Civil Engineering Department, National Institute of Technology,
Raipur (C.G.), 492010, India

⁵ Assistant Professor, Civil Engineering Department, Kalinga University, Raipur (C.G.),
492101, India

(*) *ravi.and@lic.du.ac.in*

Research Article – Available at <http://larhyss.net/ojs/index.php/larhyss/index>

Received August 7, 2024, Received in revised form May 22, 2025, Accepted May 24, 2025

ABSTRACT

Flooding is a common issue along the eastern coast of India, particularly in the lower Yerrakalava River Basin, which spans 2,402 km² and forms part of the Kolleru-Upputeru watershed. Despite the frequent flooding, this region lacks a practical flood analysis model. Therefore, we selected the Yerrakalava River Basin for hydrological modeling research. We developed the HEC-HMS Event Hydrological model for this area using a spatial database that included rainfall, soil types, slopes, drainage networks, geology, geomorphology, and land use/cover data. The model includes validation, calibration, sensitivity analysis, and flood predictions. HEC-HMS primarily generates key input parameters for the model, with tools like HEC-GeoHMS and ArcGIS 9.3 supporting the process. The calibration focused on factors such as the recession constant, threshold base flow, and Muskingum K. After calibration and validation, the model was considered effective when the efficiency value exceeded 0.82. The HEC-HMS model did a great job of simulating the hydrology of the Yerrakalava River Basin when it was used with the Thiessen polygon rainfall method, the SCS transform, recession base flow, Muskingum routing, and daily rainfall data. Results highlight the significant influence of curve numbers on the model's output.

Keywords: Yerrakalava River Basin, Watershed, Flooding, Hydrological Model, HEC – HMS Model.

Abbreviation

HEC-HMS	Hydrological Engineering Center- Hydrological Modeling System
HEC-RAS	Hydrological Engineering Center – River Analysis System
HRAP	Hydrologic Rainfall Analysis Project
HSG	Hydrological Soil Groups
HSPF	Hydrological Simulation Program-Fortran
HBV	Hydrologiska Byråns Vattenbalansavdelning
EPA	Environmental Protection Agency
ERDAS	Earth Resources Data Analysis System
ET	Evapotranspiration
ETM	Enhanced Thematic Mapper
EV	Explained Variance
FCC	False Color Composite
GeoHMS	Geoprocessing Hydrological Modeling System
GIS	Geographic Information System
GLEAMS	Groundwater Loading Effects of Agricultural Management System
GPS	Global Positioning System
U/P	Upstream
D/S	Downstream

INTRODUCTION

Recent advancements in Geographic Information Systems (GIS) have significantly contributed to the development of hydrological models for watershed systems (Anderson et al., 2002; Tandel et al., 2023; Dhiwar et al., 2021). Combining GIS technology with hydrological modeling tools provides a cost-effective solution for conducting watershed studies by facilitating data sharing and integration (Dervos and Mimikou, 2024; Verma et al., 2022a). GIS software makes it easier to make both lumped and distributed hydrological parameters through spatial analysis, which is faster and more accurate than the old ways of doing things (Srinivasa, 2010; Verma et al., 2022b). It is worth noting that GIS software has always contributed to the improvement of many fields such as hydraulics (El Hmaidi et al., 2015; Koussa and Berhail, 2021; Zegait et al., 2021).

Asia experiences the highest per capita rate of fatal weather-related disasters globally, accounting for more such events than any other continent (Mays et al., 1988; Verma et al., 2022c; Abd Rahman et al., 2023). The region's vast and diverse geography, encompassing numerous river basins and floodplains, makes it highly susceptible to natural disasters (Tucci et al., 2008; Hafnaoui et al., 2023; Verma et al., 2024a). Additionally, densely populated areas in disaster-prone regions further exacerbate vulnerability (Rasmussen et al., 1986a; Verma et al., 2024b; Verma et al., 2024c; Mehta et al., 2023).

Weather-related disasters include both floods and droughts, which affect countries throughout the world, particularly Africa where the most regions are in arid and semi-arid states (Derdour et al., 2017; Bouguerra and Benslimane, 2017; N’Guessan Bi et al., 2020;

Doumounia et al., 2020). Floods and droughts are caused by climate change (Kouassi et al., 2013; Benkhaled et al., 2013; Assemanian et al., 2021), and not only cause human disasters but also affect water resources (Nichane and Khelil, 2015; Remini, 2020; Chadee et al., 2023; Nakou et al., 2023; Remini, 2023). For these reasons, it is more than essential to find adequate solutions to mitigate, master, and manage the effects of floods and drought, analyzing the climate regionalization (Ayari et al., 2016; Bekhira et al., 2019; Cherki, 2019; Hountondji et al., 2019; Kouao et al., 2020; Zegait and Pizzo, 2023; Trivedi and Suryanarayana, 2023; Verma et al., 2023; Ben Said et al., 2024; Shaikh et al., 2024; Mehta and Yadav, 2024), propose effective preventive scenarios to improve the quality of predictions of heavy rains that cause flooding (Gassi and Saoudi, 2023), anticipate risks (Nezzal et al., 2015; Aroua, 2020; Benslimane et al., 2020), provide a comprehensive and advanced examination of flood frequency analysis (FFA) (Rao and Hamed, 2001; Hachemi and Benkhaled, 2016), determining the most robust intensity-duration-frequency (IDF) model (Houichi, 2017), focusing on the influence of the hydrographic networks structure on the hydrologic response during episodes of flooding for watersheds (Abdeddaim and Benkhaled, 2016), stormwater runoff management (Mah et al., 2023), and develop a regional climate model to assess flood risks (Pang and Tan, 2023). Floods must also be exploited through effective hydro-agricultural planning, with the functions of Irrigation, Recharge, and Security (IRS) (Bemmoussat et al., 2017; Remini, 2019; Qureshi et al., 2024)

For the Yerrakalava River Basin, there is currently no established hydrological model to analyze and understand its hydrological processes (Zhang et al., 2013; Azharuddin et al., 2022; Sahu et al., 2022; Chadee et al., 2021). Frequent flooding in the lower basin areas causes significant agricultural damage (Pellejera et al., 2011; Sahu et al., 2024). GIS software has made complex modeling easier by letting us do things like spatial overlays to figure out hydrological parameters that are important for calculations that are done on a basin-wide or grid-based level.

Various studies have demonstrated the capabilities of remote sensing (RS) and GIS in hydrology and environmental assessments (Kerboub et al., 2016; Faregh and Benkhaled, 2016; Saidi et al., 2016; Samaké et al., 2021; Jaiswal et al., 2023; Deb, 2024). Yuksel et al., (2008) utilized RS and GIS to identify erosion-prone areas in Turkey's Kartalkaya Dam region. Similarly, Ray and Dadhwal (2001) used these tools to estimate seasonal crop evapotranspiration in the Mahi Right Bank Canal. Collischonn et al., (2008) employed Tropical Rainfall Measuring Mission (TRMM) satellite data to model hydrology in the Amazon basin (Al-Abed et al., 2005).

Hydrological models simplify the complex processes within watersheds, enabling researchers to explore how they respond to various inputs (Kang and Ramírez, 2007; Chibane and Ali-Rahmani, 2015; Djellouli et al., 2015; Abdi and Meddi, 2015). The history of hydrological modeling dates back to the 19th century, rooted in civil engineering advancements for designing infrastructure like drainage systems (Baudhanwala et al., 2023; Mah et al., 2024), bridges, canals, and water supply systems (Gupta et al., 1999; Boutebba et al., 2014; Patel and Mehta, 2022; Pandey et al., 2022; Kouloughli and Telli, 2023). Initially, these models focused on conceptualizing

components of the hydrological cycle, including overland and channel flow, infiltration, evaporation, and subsurface flow (Singh and Woolhiser, 2002; Chadee et al., 2024).

The evolution of mathematical modeling began with approaches such as Mulvaney's (1850) rational method and event-based models, which linked storm runoff peaks to rainfall intensity (Singh and Woolhiser, 2002). Green and Ampt (1911) developed an infiltration capacity rate formula, while studies by Richardson (1931), Cummings (1935), Boutoutaou et al. (2020), and Remini (2024), explored the drying up of the lakes and their evaporation. Penman (1948) and Thornthwaite (1948) advanced evapotranspiration models significantly (Jensen, 2001). Other relevant research has been conducted on evapotranspiration estimation using the well-known GR2M hydrological model, or remote sensing (RS) and Mapping Evapotranspiration at high Resolution with Internalized Calibration, known as METRIC (Hamimed et al., 2017; Soro et al., 2018). Horton (1919) also devised empirical methods for estimating storm interception across various vegetation types, while many studies assessed the performance of green roofs in managing stormwater runoff using the Storm Water Management Model (SWMM). The research focuses on the green roof's ability to reduce peak discharge and delay runoff, contributing to urban flood mitigation strategies (Bentalha, 2023).

In other hand, many researches investigate how different rainfall intensities influence runoff initiation times and volumes in various soil types and land uses. The findings highlight the direct correlation between increased rainfall intensity and accelerated runoff response, emphasizing the importance of land management in erosion control (Riahi et al., 2020).

DESCRIPTION OF CASE STUDY

The Kolleru-Upputeru watershed, located between the Krishna and Godavari River basins, encompasses the Yerrakalava River basin. This basin primarily spans the West Godavari district of Andhra Pradesh, with a small portion extending into the Khammam district of Telangana. The deltaic area and the uplands divide the West Godavari district along Andhra Pradesh's eastern coast into two main physiographic regions. The Godavari and Tammileru rivers cause flooding in the western part of the district (Anderson et al., 2002). The Yerrakalava and Gunderu rivers flow from the northern parts of the basin toward the south, ultimately converging at Nandamuru village (Anil et al., 2011). The Yerrakalava River passes under the Nandamuru Aqueduct of the Eluru Canal and later flows into the Bay of Bengal, joining the Yanamadurru drain, previously referred to as the Yerrakalava (Baltas et al., 2007).

The Yerrakalava River basin (Fig. 1) lies between latitudes 16°51' and 17°25' N and longitudes 80°54' and 81°39' E (Bhaduri et al., 2000). The terrain's elevation varies from 10 to 731 meters above mean sea level. Survey of India topographic maps with index numbers 65C15, 65C16, 65G3, 65G4, 65G7, 65G8, 65G12, 65H5, and 65H9 map the study area at a 1: 50,000 scale. The northeastern part of the region has the highest elevation, while the southern part is the lowest. According to district statistics, major

crops cultivated in the area include paddy (34.5%), sugarcane (13.76%), and oilseeds (13.69%).

The Yerrakalava River and its tributaries, including Jalleru, Jalavagu, Baineru, and Turpukalava, drain the basin. Bosch and Hewlett (1982) constructed a significant reservoir near Jangareddygudem, where the Jalleru and Yerrakalava rivers meet. Constructed in 1988, the reservoir boasts a gross storage capacity of 155.4 million cubic meters, designed to regulate a flood discharge of 1370.5 cubic meters per second. The reservoir irrigates approximately 24,700 acres of land and provides a flood control capacity of 3 TMC (Dadhwai, 2001; Kumar et al., 2008).

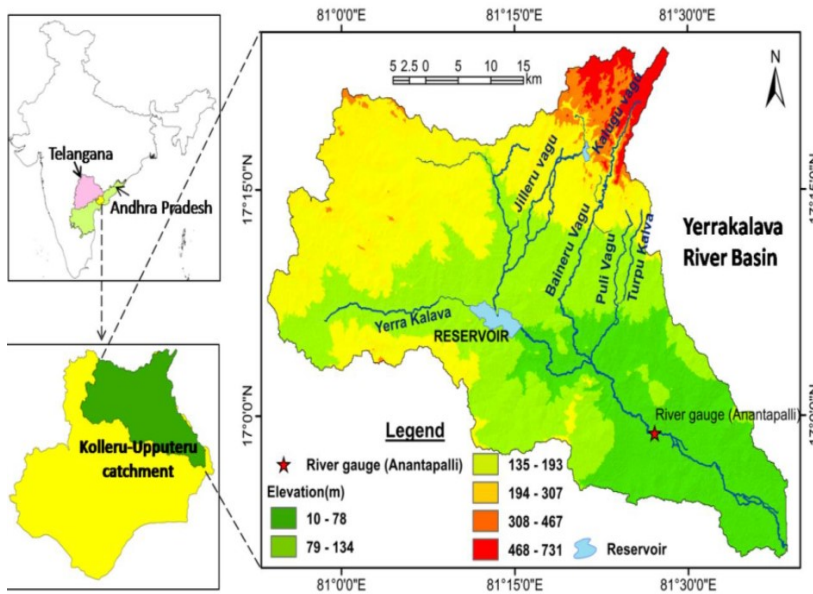


Figure 1: A map showing the location of the Yerrakalava River Basin

MATERIAL AND METHODS

Sample Collection

Topo sheets were a fundamental source of data on drainage, transportation networks, and land use/land cover. Field observations and satellite imagery validated and updated this information (Brath et al., 2006). Utilizing fieldwork and satellite data processed with remote sensing (RS) and geographic information system (GIS) methodologies, the boundaries of the study area were refined (Young et al., 2015). We developed the district's geological map by combining remote sensing data, selected field observations, and topo sheets from the Geological Survey of India, and generated the soil map of the Yerrakalava

River Basin using data from the National Bureau of Soil Survey and Land Use Planning. Spatial databases for these tasks were created using ArcGIS and ERDAS software.

The study utilized rainfall data from 14 rain gauge stations located at mandal headquarters across the region (Candela et al., 2012). Daily rainfall records spanning 1990 to 2024 were analyzed, focusing on the spatial distribution of average monthly and annual rainfall across the Yerrakalava Basin. The hydrological modeling was conducted using the Hydrological Engineering Center-Hydrological Modeling System (HEC-HMS), developed by the US Army Corps of Engineers (Van Chinh et al., 2013; Fernando et al., 2021; Atallah et al., 2024; Mehta and Yadav, 2024; Kherde et al., 2024).

The model underwent verification and calibration for several rainfall events occurring between 2006 and 2024 (Choudhury et al., 2002). Cunderlik and Simonovic (2004) employed performance metrics to assess the accuracy of the model and evaluate the sensitivity of input parameters under varying conditions. Geomorphological features were characterized through a combination of remote sensing data, contour information from topo sheets, and limited field observations.

Analysis of Surface and sub-surface water sources

Every simulation combines the control, precipitation, and basin components (Golian et al., 2011). As stated in the HEC-HMS User's Manual, all landforms within a watershed consist of either permeable or impermeable surfaces that are structurally interconnected, as detailed in Table 1 (Gopinath et al., 2014).

HEC-HMS MODEL CONFIGURED

The Hydrological Modelling System (HEC-HMS) from the US Army Corps Hydrological Engineering Centre is the hydrological model for the research region. This model is global and local (Fleming, 2009). Applications are what motivate its usage. In HEC-HMS, a distinct sub-model represents each stage of the runoff process, including models that determine base flow, runoff generation, rainfall loss, and channel routing (Fleming, 2009). The flow diagram in Fig. 2 depicts a detailed process.

GIS hydrological models for managing water resources in the Indian Verrakalava river basin: A case study

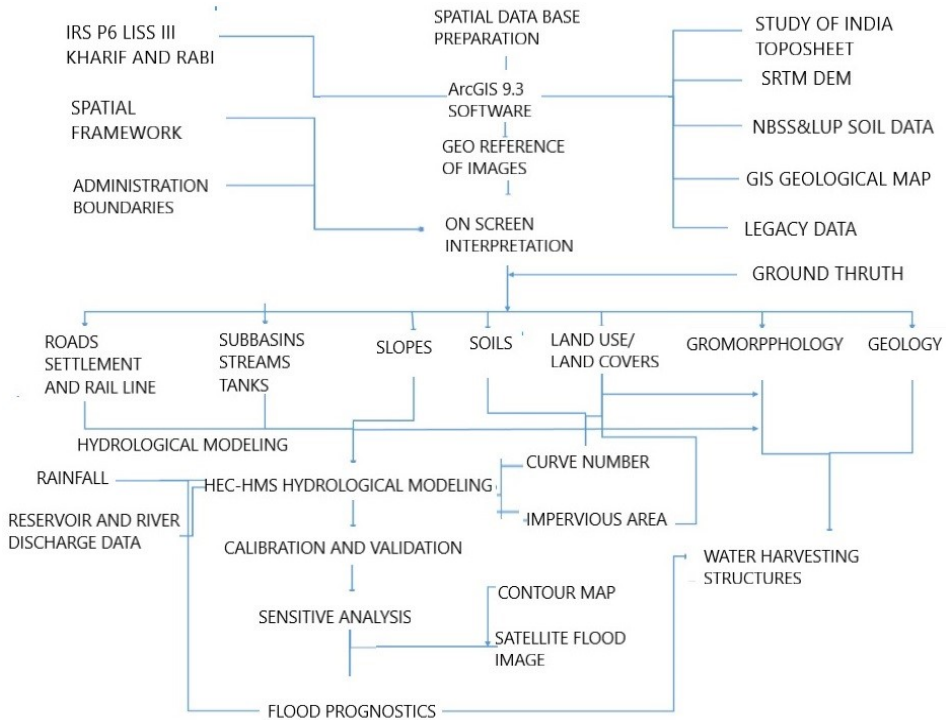


Figure 2: Flow diagram displaying an extensive process

Table 1: Physical properties were obtained using the HEC-GeoHMS model.

Data Layer	Physical Characteristics	Attribute Table Head	Hydrological Formula	References
Stream Layer	Length Up-Stream	RivLen ElevUp	$Fr_1 = \frac{V_1}{\sqrt{gy_1}} = \frac{q}{y_1 \sqrt{gy_1}}$	Yasin et al., (1988)
Sub-Basin Layer	Areas	Area	$K_c = \frac{P}{2\sqrt{\pi A}} = 0.28 \frac{P}{\sqrt{A}}$	Golian et al., (2011)
Centroid Layer	Centroid Location. Centroid Elevation.	Elevation	$Hmed = \frac{\sum(h_i \cdot S_i)}{A}$	Golian et al., (2011)
Longest Flow Path Layer	Location of Longest Flow Path	Longest FL.	$T_{sh} = \frac{0.007 (nL)^{0.8}}{(P_2)^{0.5} S^{0.4}}$	Baltas et al., (2007)

Basin Model

The primary data sources for the study include basin information, land use/cover, and soil texture, all of which are key characteristics derived from the Digital Elevation Model (DEM). The DEM, generated using 90-meter resolution data from the Shuttle Radar Topographic Mission (SRTM) (Rawat et al., 2014), is processed using the HEC-GeoHMS GIS pre-processor in combination with ArcGIS software. This segmentation of the watershed into multiple interconnected sub-basins effectively simulates the stream network (Tibangayuka et al., 2022).

The Consultative Group for the International Agricultural Research Consortium of Spatial Information provides public access to the data (Ahmed, 2009). The study area is located in Zone 44 of the Universal Transverse Mercator (UTM) projection system. ArcGIS software delineates the specific region of interest based on its boundaries. Fig. 3 outlines the sequential steps involved in generating the drainage system for the study area (Jafarzadegan and Merwade, 2017).

Comparing the drainage derived from topographic maps with the digital elevation model yields highly accurate results (Fereshtehpour et al., 2024). Consequently, the current HEC-HMS modeling study employs the SRTM DEM with a 90-meter resolution. The HEC-GeoHMS tool in ArcGIS analyzes stream data from the study area to determine the number of sub-basins, leading to the formation of 12 interconnected sub-basins (Rao et al., 2011). These sub-basins, along with the drainage network and topographical attributes, serve as inputs for the HEC-HMS model. Fig. 4 illustrates the final drainage network and sub-basin delineations produced by the HEC-HMS model (Valencia Ortiz, and Martínez-Graña, 2024).

Curve Number Generation

The Soil Conservation Service (SCS) simplified the combined impacts of soil types, watershed features, and land use into a single parameter known as the curve number (CN). According to Lerat et al., (2012), this parameter reflects the potential runoff from a hydrologic soil-cover complex. Watersheds with diverse land uses and soil types assign a specific runoff curve number based on each unique combination of land use and soil type (Maity et al., 2013). Water resource projects worldwide widely adopt the SCS curve number. It is particularly popular in Mediterranean regions for practical flood modeling applications (Tramblay et al., 2011). Once we determine individual curve numbers, we can use the following relationship to calculate the weighted curve number.

$$CN = \frac{\sum(CN_1 \times a_1 + CN_2 \times a_2 + \dots + CN_n \times a_n)}{\sum a} \quad (1)$$

The weighted curve number (CN) is calculated using the formula where a_i represents the area of a specific land unit, $\sum a$ denotes the total area, and CN_1, CN_2, CN_n is the curve number for land unit 1 (Meenu et al., 2012). Consider two polygons from the previous example, each with areas of 30 and 40 hectares and corresponding curve numbers of 79 and 89. Applying this relationship, the resulting

weighted curve is 84.7. This process is repeated for every sub-basin to derive a weighted curve number. Fig. 5 illustrates the curve number map under moderate conditions.

Loss Model

The HEC-HMS model incorporates three key parameters: the curve number, the impervious percentage, and the initial abstraction (loss) as defined by the SCS loss method. According to USACE (Koneti et al., 2018), the model utilizes these parameters in Eq. (2).

$$P_e = \frac{(p-I_a)^2}{p-I_a+S} \quad (2)$$

P represents the total rainfall, I_a denotes the initial abstraction, S is the watershed's maximum potential retention or storage capacity, and P_e is the cumulative excess rainfall or direct runoff (Niehoff et al., 2002). The SCS established an empirical relationship between I_a and S based on multiple experimental analyses, expressed as $I_a = 0.2S$. Here, S corresponds to the maximum storage capacity of the catchment (in mm), derived using the specified formula and the curve number (CN) in Eq. (3). Based on rainfall records, soil texture, antecedent moisture condition, and land use/cover were used to calculate the curve number values.

$$S = \frac{25400}{CN} - 254 \quad (3)$$

The lumped curve number for individual sub-basins varies between 48.3 and 73.4. Land use/land cover information provided the impervious data needed for the loss model (Golian et al., 2011). Papathanasiou et al., (2015) classified all artificial structures within the research area, including roads and buildings, as impermeable zones for this study. These impermeable areas disrupt the water cycle and hinder natural drainage, increasing the community's susceptibility to flooding (Ranzi et al., 2002). The proportion of impermeable surfaces within the study area ranges from 6.2% to 14.1% (Sharma and Kujur, 2012).

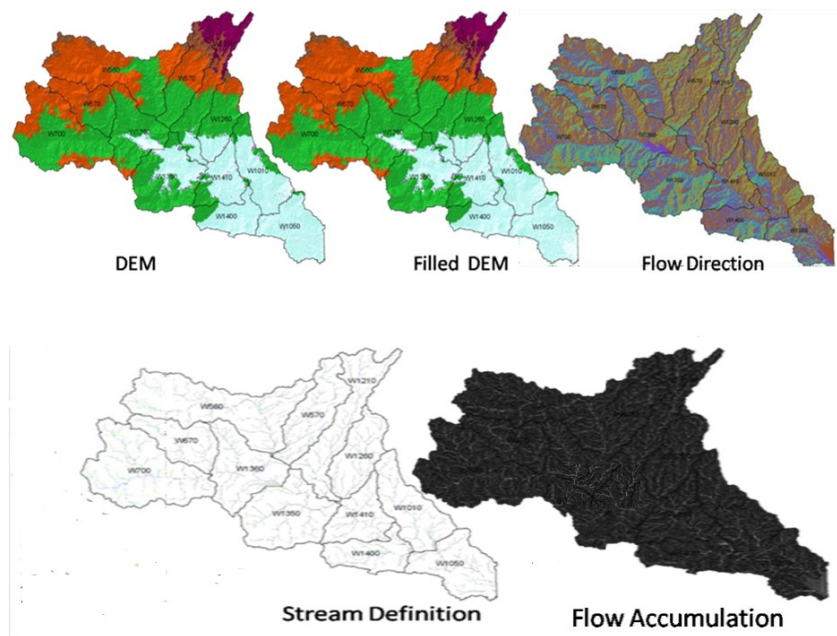


Figure 3: Sequential steps involved for creating the drainage system for the study area

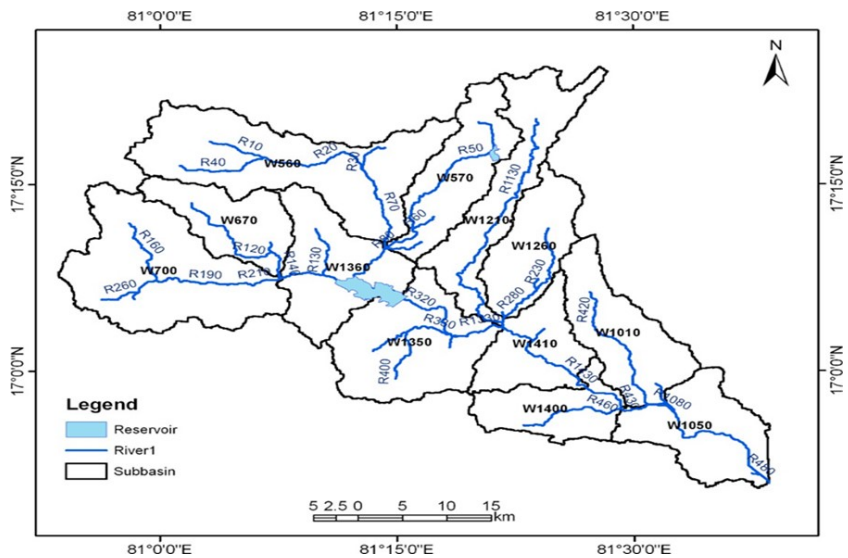


Figure 4: Study area drainage network and sub-basin delineations

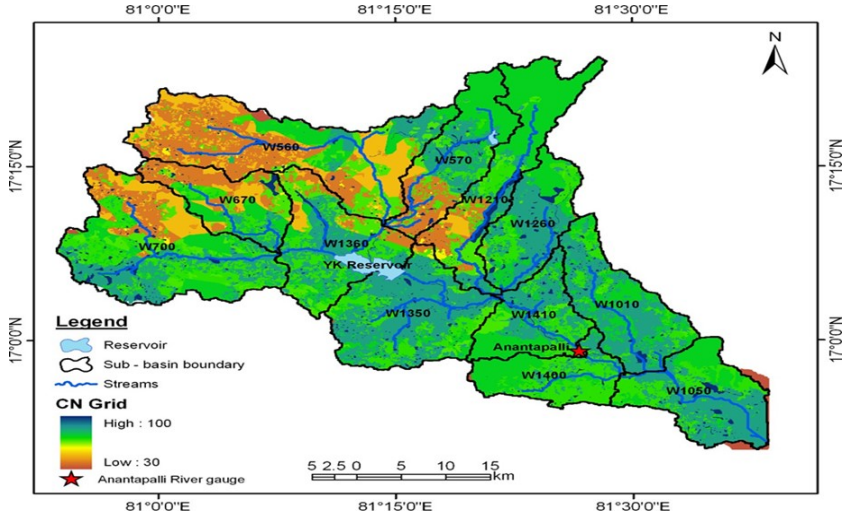


Figure 5: Curve number map under moderate conditions

RESULTS AND DISCUSSION

Transform Model

Dadhwal (2001) suggests using the SCS Unit Hydrograph method to effectively estimate the excess precipitation contributing to surface runoff within the study area. The transform model in the HEC-HMS software implements this approach. Roy et al., (2013) describe how to use the HEC-GeoHMS CN lag method tool to determine the basin lag time.

$$Lag = \frac{L^{0.8} \times \left(\left(\frac{100}{CN} - 10 \right) + 1 \right)^{0.7}}{1900 \times Y^{0.5}} \quad (4)$$

The hourly basin lag time, represented as "lag," is determined by the hydraulic length of the watershed (L, measured in feet) and the basin slope fraction (Y). In the Verrakalava River basin, the standard curve number values range between 49 and 73, as noted by Samanta and Paul (2016). Golian et al., (2011) cited research by the Natural Resource Conservation Service, which established a correlation between the unit hydrograph (UH) peak and its timing.

$$U_p = C \frac{A}{T_p} \quad (5)$$

C, representing the conversion constant of 2.08 in the SI system, and A, denoting the watershed area are key parameters. The duration of the additional precipitation unit influences the peak time, also known as the time of ascension (Sharma and Kujur, 2012).

$$T_P = \frac{ot}{2} + t_{lag} \tag{6}$$

The basin lag (y) represents the time difference between the peak of the unit hydrograph (UH) and the centroid of the surplus rainfall. The period of excess precipitation (p), which also serves as the computational interval for the analysis, is crucial (Agarwal et al., 2013). To determine the basin lag, it is essential to know the curve number (CN) and the slope of the sub-basin (Basin Slope) (Singh and Woolhiser, 2002). The SCS transform algorithm utilizes the calculated lag time to incorporate the characteristics of the study area's sub-basins, as outlined in Table 2.

Table 2: Characteristics of the research area's sub-basin

Statistical analysis

The smallest drainage areas are found in sub-basins W1400 (121.1 km²), W670 (134.1 km²), and W1410 (131.5 km²), while the largest drainage areas are observed in sub-basins W560 (358 km²) and W700 (329 km²). The slope is lowest in W1050 (1.11%) and W1400 (1.22%), with W1260 reaching the highest slope of 8.23%. W1210 has the highest weighted (lumped) curve number at 73.4, while W560 has the lowest at 48.3 (Tramblay et al., 2011). W1360 exhibits the highest percentage of impermeable land at 14.1%, in contrast to W560, which has the lowest at 6.2% (Warburton et al., 2012). The lag time for W570 is 480.7 minutes, and for W560, it is 1534.4 minutes. Table 3 presents the stream parameters for the study area (Chu and Steinman, 2009). The stream network and sub-basin data, as described earlier, are extracted using HEC-Geo HMS for running the HEC-HMS model. Fig. 6 shows the unscaled map of the HEC-HMS model for the Yerrakalava River Basin and its twelve sub-basins.

GIS hydrological models for managing water resources in the Indian Verrakalava river basin: A case study

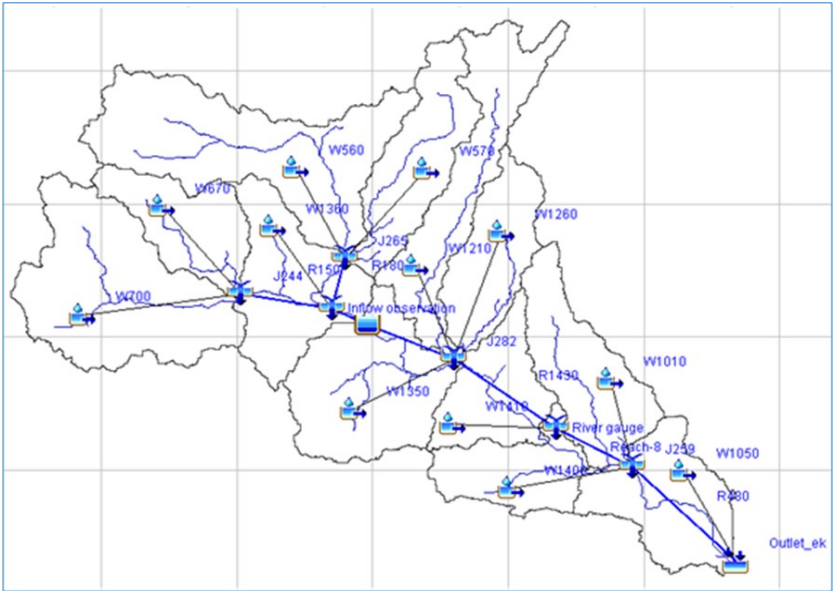


Figure 6: Yerrakalava River Basin in HEC-HMS model

Table 3: Study area's stream parameters

Stream Name	Slope (%)	Elevation U/P (m)	Elevation D/S (m)	River Length (m)	Stream Name	Slope (%)	Elevation U/P (m)	Elevation D/S (m)	River Length (m)
R10	0.0008	57.00	56.00	1294.26	R340	0.0037	188.00	161.00	7239.88
R20	0.0007	49.00	46.00	4153.16	R360	0.0022	161.00	129.00	14717.64
R30	0.0012	49.00	46.00	2464.19	R370	0.0034	147.00	129.00	5278.16
R40	0.0029	63.00	56.00	2380.04	R380	0.0026	190.00	161.00	11218.71
R50	0.0030	85.00	68.00	5603.19	R390	0.0068	277.00	111.00	24399.95
R60	0.0027	91.00	68.00	8521.36	R400	0.0038	125.00	111.00	3649.81
R70	0.0012	29.00	25.00	3306.14	R410	0.0024	129.00	96.00	13735.43
R80	0.0019	71.00	25.00	23650.83	R420	0.0027	111.00	96.00	5501.39
R90	0.0020	56.00	29.00	13572.75	R460	0.0236	96.00	95.00	42.43
R100	0.0010	14.00	13.00	1038.20	R470	0.0018	104.00	95.00	5040.11
R110	0.0005	23.00	13.00	18260.13	R480	0.0022	116.00	112.00	1837.02
R120	-0.0012	13.00	15.00	1648.86	R490	0.0039	174.00	112.00	16066.83
R130	0.0000	25.00	25.00	84.85	R450	0.0037	115.00	84.00	8364.44
R140	0.0011	25.00	23.00	1770.37	R1030	0.0038	112.00	93.00	4985.88
R150	0.0000	29.00	29.00	84.85	R440	0.0016	93.00	84.00	5482.20
R160	0.0008	29.00	23.00	7259.85	R1080	0.0036	151.00	110.00	11414.51
R170	0.0082	404.00	54.00	42893.69	R1130	0.0011	84.00	79.00	4632.79
R180	0.0046	53.00	51.00	434.56	R1170	0.0021	95.00	79.00	7708.08
R190	0.0038	51.00	49.00	531.84	R310	0.0012	110.00	99.00	9561.69
R200	0.0167	54.00	52.00	120.00	R290	0.0084	101.00	99.00	238.49
R210	-0.0032	52.00	53.00	312.43	R1230	0.0009	99.00	93.00	6885.29
R220	0.0000	55.00	55.00	169.71	R1270	0.0029	80.00	74.00	2103.82
R230	0.0023	55.00	53.00	852.43	R300	0.0039	118.00	74.00	11297.53
R240	0.0000	49.00	49.00	60.00	R350	0.0013	114.00	110.00	3147.35
R250	0.0011	56.00	49.00	6491.39	R1330	-0.0015	112.00	114.00	1319.74
R260	0.0000	79.00	79.00	5671.98	R1370	0.0015	121.00	114.00	4788.56
R270	0.0020	79.00	57.00	10734.18	R320	0.0032	58.00	55.00	930.62
R280	0.0013	37.00	29.00	5981.03	R430	0.0029	74.00	55.00	6446.83
R330	0.0007	46.00	37.00	12297.93	R1430	0.0018	68.00	57.00	6158.38

Validation of the HEC-HMS model

The initial abstraction represents the amount of precipitation required for surface runoff to take place. The initial abstraction is adjusted by different scenarios of $\pm 10\%$, $\pm 20\%$, and $\pm 30\%$, while other model parameters remain constant (Kang and Ramírez, 2007). The model is then executed under these varied abstraction conditions, and the resulting hydrographs are compared with the baseline hydrographs shown in Fig. 7 (Joo et al., 2014). The runoff (m^3/s) is plotted on the Y-axis, and the date is shown on the X-axis. As observed in Fig. 7, an increase in I_a leads to a reduction in stream flow on the rising limb (Gopinath et al., 2014). Table 4 illustrates the variation in stream flow when I_a is altered by -30% to $+30\%$ (Golian et al., 2011).

Table 4: Stream flow (m^3/s) due to a change in initial abstraction

Date	Baseline	-30 %	-20 %	-10 %	+10 %	+20 %	+30 %
Oct. 2, 2024	25.8	25.8	25.8	25.8	25.8	25.8	25.8
Oct. 3, 2024	15.6	15.6	15.6	15.6	15.6	15.6	15.6
Oct. 4, 2024	8.7	9.6	9	8.7	8.7	8.7	8.7
Oct. 5, 2024	166	185.6	179.1	172.6	159.6	153.3	147.1
Oct. 6, 2024	292.1	308.8	303.3	297.8	286.3	280.6	275
Oct. 7, 2024	105.7	107	106.6	106.1	105.2	104.6	104
Oct. 8, 2024	24.6	27.6	26.6	25.6	23.6	22.6	21.6
Oct. 9, 2024	43.6	42.9	43.1	43.3	43.8	44	44.1
Oct. 10, 2024	10	11.3	10.9	10.4	9.6	9.2	8.8

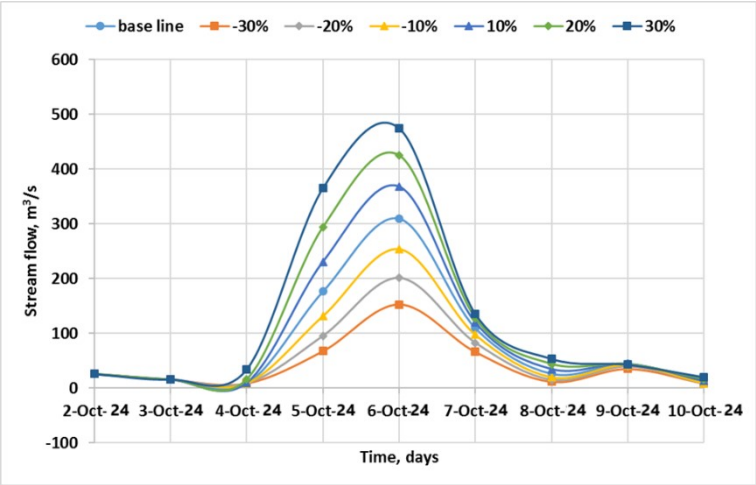


Figure 7: Event model sensitivity on the curve number of stream flow

The rainfall distribution over several months, as observed through various rain gauge stations. High-elevation regions receive more rainfall compared to low-elevation areas (Table 5). The areas with the highest rainfall in the basin are the rain gauges at Dommapeta and Buttayagudem, both located in elevated, forested regions (Sempere Torres, 2001). This indicates that the lower basin, with its intense rainfall, is more prone to flooding (Choudhury et al., 2002). The study region's vulnerability has increased over the years, driven by higher rainfall in the upper basin and increased rainfall intensity in the lower basin (Choudhury et al., 2002). HEC-HMS Event Model to the Yerrakalava River Basin, incorporating methods such as SCS loss, SCS transform, recession base flow, and Muskingum routing. During calibration and validation, the Nash-Sutcliffe Model Efficiency (NSE) values were 0.865 and 0.826, respectively, confirming the robustness of the model. These findings support the conclusion that the model applies to the Yerrakalava River Basin (Candela et al., 2012). Furthermore, the peak discharge deviation during both calibration and validation was less than 5%, except in one instance (Candela et al., 2012). Fig. 8 demonstrates the accuracy of the peak discharge prediction, making it suitable for flood forecasting studies (Abushandi, 2013). All events showed a peak deviation of zero, meaning the peak timing aligns perfectly with the observed data (Soni et al., 2023). Furthermore, the study area accurately recognizes the flood volume with a volume deviation of less than 20% (Anbazhagan et al., 2005).

Table 5: Shows the Yerrakalava River Basin's average monthly rainfall (mm) from various rain gauges

Name-of-the-Mandal	Height(m)	Jan	Feb	Mar	Apr	May	Jun	Jul	Aug	Sep	Oct	Nov	Dec
Aswaraopeta	180	8.6	5.6	12.3	15.4	72.3	136.2	270.1	284.1	162.3	110.6	37.4	12.4
Buttayagudem	135	5.8	9.3	14.8	13.2	61.3	151.7	290.4	310.9	188.3	141.0	39.2	12.2
Chintalapudi	139	12.7	7.9	20.3	23.8	62.7	136.0	256.0	274.0	165.4	141.6	39.5	12.0
Devarapalli	58	4.2	5.6	15.3	10.0	45.6	103.6	197.0	196.0	159.7	133.5	40.1	14.3
Dommapeta	214	8.7	10.0	14.1	23.7	78.1	152.4	303.7	314.6	199.6	119.1	53.2	11.3
Tirumala	100	7.8	5.8	26.4	11.7	60.6	120.4	225.0	236.3	180.8	126.3	45.5	13.1
Gopalapuram	55	10.5	6.7	15.9	11.9	61.5	134.3	229.8	210.6	180.0	136.2	32.6	16.0
Jangareddi-Gudem	96	5.6	7.0	19.2	18.3	56.0	152.7	257.5	252.0	189.6	140.3	44.1	12.0
Jilugumilli	157	8.3	6.8	17.2	16.0	57.3	135.0	254.0	279.1	165.7	116.5	38.4	10.2
Kamavarapu-Kota	113	7.6	8.0	24.2	10.6	65.1	122.1	223.6	256.5	183.4	121.7	36.9	9.7
Koyyalagudem	92	9.6	7.8	15.7	10.6	53.2	141.2	259.4	259.0	200.3	143.5	43.2	12.0
Nallagerla	51	8.1	5.8	13.0	11.8	60.2	115.4	208.6	231.3	174.4	142.4	40.0	13.1
Nidadavolu	24	7.3	5.7	11.7	21.1	69.7	127.5	207.2	226.2	174.7	155.1	63.3	11.7
Narasapuram	122	7.5	8.2	15.0	18.1	58.6	121.5	230.7	254.6	141.8	114.4	35.2	10.8
Average	8.0	7.2	16.8	15.4	61.6	132.1	243.8	256.1	176.1	131.6	42.0	12.2	
Min	4.2	5.6	11.7	10.0	45.6	103.6	197.0	196.0	141.8	110.6	32.6	9.7	
Max	12.7	10.0	26.4	23.8	78.1	152.7	303.7	314.6	200.3	155.1	63.3	16.0	

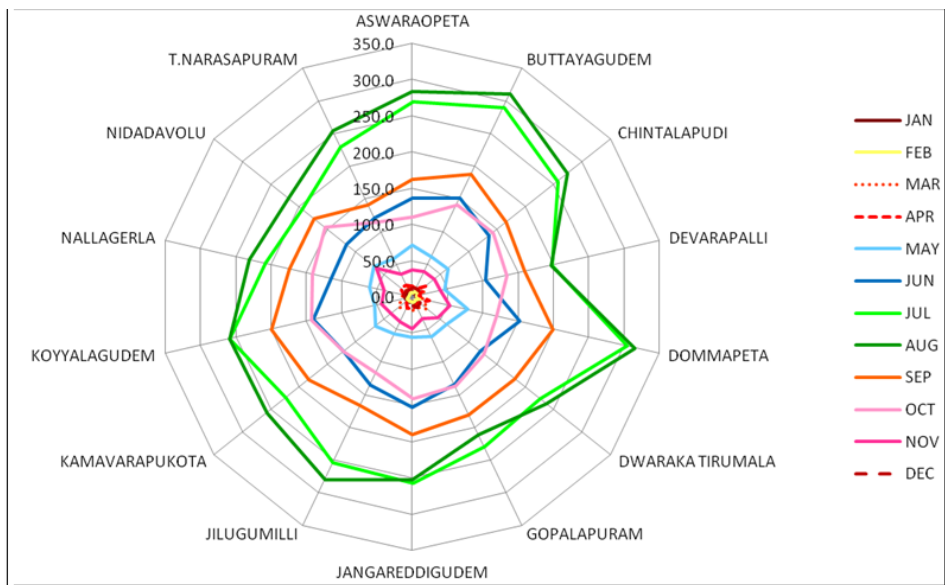


Figure 8: The distribution of various rain gauges' average monthly rainfall

CONCLUSIONS

The sensitivity analysis of the model with seven factors reveals that the curve number plays a crucial role. A $\pm 30\%$ variation in the curve number leads to a significant change in peak discharge, exceeding 50%. As the curve number increases, both peak discharge and flood volume increase and vice versa. Other factors like initial abstraction, impervious area, base flow threshold ratio, recession constant, Muskingum K, and basin lag have a smaller effect on the model. When these factors change, they only cause a 6% change in peak discharge and volume. The Curve Number, which reflects soil type, antecedent moisture conditions, and land use/cover, makes the model particularly sensitive to these factors. In the Yerrakalava River watershed, land use and cover significantly influence flow, as soil type remains constant over time. We have identified a potential reservoir location at the confluence of the Yerrakalava, Baineru, and Turpukalava rivers to manage floodwaters from the upper basin, based on the thematic maps created.

A 30% increase in rainfall results in a flood inundation area of 12,213 acres of agricultural land, exceeding the baseline inundation area of 9,475.6 acres. Runoff analysis of the sub-basins indicates that the upper reaches of the Yerrakalava River Basin are the primary contributors to flooding. Specifically, the sub-basins W1210 and W1260, located just below the Yerrakalava Reservoir on the northeastern edge, are identified as responsible for the largest peak floods, and these areas lack flood control measures. The HEC-HMS model is currently simulated on a daily rainfall time step, but performing the simulation on an hourly basis is recommended to pinpoint the exact timing of the peak flood.

Running the HEC-HMS model for past land use/land cover scenarios is suggested to predict future conditions using techniques like the Cellular Automata-Markov model, as the model is highly sensitive to curve numbers. For future studies, using river hydraulic models such as HEC-RAS is recommended to accurately assess flood inundation in lower areas.

FUTURE SCOPE OF THE STUDY

The rainfall increments for the selected event of August 2008 are assumed to be 10%, 20%, and 30%. Corresponding to these increments, the peak discharges are calculated as 972.2 m³/s, 1047.3 m³/s, and 1122.2 m³/s, respectively. A 10% increase in rainfall results in flood submergence of 10,388 acres, representing a 9.6% increase compared to the baseline inundation area of 9,475.6 acres. For 20% and 30% rainfall increases, the flood submergence areas expand to 11,302 acres and 12,213 acres, indicating a 19.6% and 28.8% rise in flooded areas, respectively. Sub-basin rainfall analysis shows an increasing trend across most sub-basins. Consequently, the model is projected for future scenarios with higher rainfall increments, considering the current land use, land cover, and soil conditions.

LIMITATIONS OF THE STUDY

The research focuses on the preparation and analysis of a spatial database containing information on rainfall, drainage, geology, geomorphology, soil, slope, and land use/land cover. We employed methods like visual image interpretation and digitization, along with spatial analysis tools in ArcGIS 9.3, to create the spatial database for the Yerrakalava River Basin. We then used this database as input for the HEC-HMS hydrological model. We conducted flood forecasting studies using satellite data to estimate the submergence area for various rainfall events. The analysis included determining the threshold peak flood at the Anantapalli river gauge, which is responsible for flood submergence in the basin's lower regions; assessing rainfall characteristics and trends across different sub-basins; estimating the expanded inundation area in response to increased rainfall; evaluating runoff from various sub-basins contributing to flood submergence; and recommending appropriate flood control structures.

Declaration of competing interest

The authors declare that they have no known competing financial interests or personal relationships that could have appeared to influence the work reported in this paper.

REFERENCES

- ABDEDDAIM H., BENKHALED A. (2016). Influence of the hydrographic network on hydrologic response in northeast watersheds of Algeria, *Larhyss Journal*, No 27, pp. 313-335. (In French)
- ABDI I., MEDDI M. (2015). Rainfall-runoff modeling distributed in two watersheds in eastern Algeria, *Larhyss Journal*, No 23, pp. 7-22. (In French)
- ABD RAHMAN A.N., OTHMAN F., WAN JAAFAR W.J., AHMED ELSHAFIE A.H.K. (2023). An assessment of floods' characteristics and patterns in Pahang, Malaysia, *Larhyss Journal*, No 55, pp. 89-105.
- ABUSHANDI E., MERKEL B. (2013). Modelling rainfall runoff relations using HEC-HMS and IHACRES for a single rain event in an arid region of Jordan, *Water resources management*, Vol. 27, Issue 2, pp. 2391-2409.
<https://doi.org/10.1007/s11269-013-0293-4>
- AGARWAL R., GARG P.K., GARG R.D. (2013). Remote sensing and GIS based approach for identification of artificial recharge sites, *Water resources management*, Vol. 27, Issue 2, pp. 2671-2689.
<https://doi.org/10.1007/s11269-013-0310-7>
- AL-ABED N., ABDULLA F., ABU KHYARAH A. (2005). GIS-hydrological models for managing water resources in the Zarqa River basin, *Environmental Geology*, Vol. 47, Issue 1, pp. 405-411. <https://doi.org/10.1007/s00254-004-1165-2>
- ANBAZHAGAN S., RAMASAMY S.M., DAS GUPTA S. (2005). Remote sensing and GIS for artificial recharge study, runoff estimation and planning in Ayyar basin, Tamil Nadu, India, *Environmental Geology*, Vol. 48, Issue 2, pp. 158-170.
<https://doi.org/10.1007/s00254-005-1284-4>
- ANDERSON M.L., CHEN Z.Q., KAVVAS M.L., FELDMAN A. (2002). Coupling HEC-HMS with atmospheric models for prediction of watershed runoff, *Journal of Hydrologic Engineering*, Vol. 7, Issue 4, pp. 312-318.
[https://doi.org/10.1061/\(ASCE\)1084-0699\(2002\)7:4\(312\)](https://doi.org/10.1061/(ASCE)1084-0699(2002)7:4(312))
- AROUA N. (2020). Flood risk reduction strategy in Algiers a brief modern history (XVIthC -XIXthC), *Larhyss Journal*, No 43, pp. 73-89.
- ASSEMIAN A.E., DJE BI DOUTIN S., SAMAKÉ Y. (2021). Consequences of the effects of climate change on water resources in a humid tropical zone of central eastern Côte d'Ivoire, *Larhyss Journal*, No 45, pp. 95-105.
- ATALLAH M., DJELLOULI F., HAZZEB A. (2024). Rainfall-runoff modeling using the HEC-HMS model for the Mekerra wadi watershed (N-W Algeria), *Larhyss Journal*, No 57, pp. 187-208.

- AYARI K., DJEBBI M., CHAKROUN H. (2016). Flood risk mapping of the city of El Bab Medjez by the overflow of the Medjerda, *Larhyss Journal*, No 25, pp. 285-307. (In French)
- AZHARUDDIN M., VERMA S., VERMA M.K., PRASAD A.D. (2022). A synoptic-scale assessment of flood events and ENSO streamflow variability in Sheonath River Basin, India, *Advanced Modelling and Innovations in Water Resources Engineering*, Vol. 176, Issue 1, pp. 93-104. https://doi.org/10.1007/978-981-16-4629-4_8
- BALTAS E.A., DERVOS N.A., MIMIKOU M.A. (2007). Determination of the SCS initial abstraction ratio in an experimental watershed in Greece, *Hydrology and Earth System Sciences*, Vol. 11, Issue 6, pp. 1825-1829. <https://doi.org/10.5194/hess-11-1825-2007>
- BAUDHANWALA D., KANTHARIA V., PATEL D., MEHTA D., WAIKHOM S. (2023). Applicability of SWMM for urban flood forecasting a case study of the western zone of Surat city, *Larhyss Journal*, No 54, pp. 71-83.
- BEKHIRA A., HABI M., MORSLI B. (2019). The management of flood risk and development of watercourses in urban areas: case of the town of Bechar, *Larhyss Journal*, No 37, pp. 75-92. (In French)
- BEMMOUSSAT A., ADJIM M., BENSAOULA F (2017). Use of the ZYGOS model for the estimation of groundwater recharge in Sikkak watershed (Northen west of Algeria), *Larhyss Journal*, No 30, pp. 105-119. (In French)
- BENKHALED. A., REZGUI. Z., SAKHRAOUI. F. (2013). Floods in Abiod wadi: analysis of database, *Larhyss Journal*, No 14, pp. 179-191
- BEN SAID M., HAFNAOUI M.A., HACHEMI A., MADI M., BENMALEK A. (2024). Evaluating the effectiveness of the existing flood risk protection measures along wadi Deffa in El-Bayadh city, Algeria, *Larhyss Journal*, No 59, pp. 7-28.
- BENSLIMANE M., BERREKSI A., BENMAMAR S., BOUACH A. (2020). Flood risk numerical simulation of Bejaia city urban zone (Algeria), *Larhyss Journal*, No 42, pp. 167-178.
- BENTALHA C. (2023). Evaluation of the hydraulic and hydrology performance of the green roof by using SWMM, *Larhyss Journal*, No 53, pp. 61-72.
- BHADURI B., HARBOR J.O.N., ENGEL B., GROVE M. (2000). Assessing watershed-scale, long-term hydrologic impacts of land-use change using a GIS-NPS model, *Environmental management*, Vol. 26, Issue 4, pp. 643-658. <https://doi.org/10.1007/s002670010122>
- BOSCH J.M., HEWLETT J.D. (1982). A review of catchment experiments to determine the effect of vegetation changes on water yield and evapotranspiration, *Journal of hydrology*, Vol.55, Issues 1-4, pp. 3-23. [https://doi.org/10.1016/0022-1694\(82\)90117-2](https://doi.org/10.1016/0022-1694(82)90117-2)

- BOUGUERRA S.A., BENSLIMANE N. (2017). Characterization of drought weather in climate semi-arid: case of watershed wadi Boumessaoud (N-W Algeria), *Larhyss Journal*, No 29, pp. 95-110. (In French)
- BOUTEBBA K., BOUZIANE M.T., BOUAMRANE A. (2014). Decision-making aid for optimizing the management of drinking water supply networks, *Larhyss Journal*, No 20, pp. 279-296. (In French)
- BOUTOUTAOU D., ZEGGANE H., SAGGAI S. (2020). Evaporation from the water surface of lakes and reservoirs of the arid zone of the mediterranean: case of Algeria, *Larhyss Journal*, No 43, pp. 91-101.
- BRAITH A., MONTANARI A., MORETTI G. (2006). Assessing the effect on flood frequency of land use change via hydrological simulation (with uncertainty), *Journal of hydrology*, Vol. 324, Issues 1-4, pp. 141-153.
<https://doi.org/10.1016/j.jhydrol.2005.10.001>
- CANDELA L., TAMOH K., OLIVARES G., GOMEZ M. (2012). Modelling impacts of climate change on water resources in ungauged and data-scarce watersheds. Application to the Siurana catchment (NE Spain), *Science of the total environment*, Vol. 440, Issue 4, pp. 253-260. <https://doi.org/10.1016/j.scitotenv.2012.06.062>
- CHADEE A.A., CHADEE X.T., MWASHA A., MARTIN H.H. (2021). Implications of 'lock-in' on public sector project management in a small island development state, *Buildings*, Vol. 11, Issue 5, pp. 198. <https://doi.org/10.3390/buildings11050198>
- CHADEE A., RAMSUBHAG C., MOHAMMED A. (2024). Implications of Bid Rigging Practices in Small Island Developing States: A Case Study, *Asian American Research Letters Journal*, Vol. 1, Issue 4, pp. 1-28.
<https://aarlj.com/index.php/AARLJ/article/view/62>
- CHERKI K (2019). Daily and instantaneous flood forecasting using artificial neural networks in a north-west Algerian watershed, *Larhyss Journal*, No 40, pp. 27-43.
- CHIBANE B., ALI-RAHMANI S.E. (2015). Hydrological based model to estimate groundwater recharge, real- evapotranspiration and runoff in semi-arid area, *Larhyss Journal*, No 23, pp. 231-242.
- CHOUDHURY P., SHRIVASTAVA R.K., NARULKAR S.M. (2002). Flood routing in river networks using equivalent Muskingum inflow, *Journal of Hydrologic Engineering*, Vol. 7, Issue 6, pp. 413-419.
[https://doi.org/10.1061/\(ASCE\)1084-0699\(2002\)7:6\(413\)](https://doi.org/10.1061/(ASCE)1084-0699(2002)7:6(413))
- CHU X., STEINMAN A. (2009). Event and Continuous Hydrologic Modeling with HEC-HMS, *Journal of Irrigation and Drainage Engineering*, Vol.135, Issue 1, pp. 119-124.
[https://doi.org/10.1061/\(ASCE\)0733-9437\(2009\)135:1\(119\)](https://doi.org/10.1061/(ASCE)0733-9437(2009)135:1(119))
- COLLISCHONN B., COLLISCHONN W., TUCCI C.E.M. (2008). Daily hydrological modeling in the Amazon basin using TRMM rainfall, estimates, *Journal of Hydrology*, Vol. 360, Issues 1-4, pp. 207-216.

<https://doi.org/10.1016/j.jhydrol.2008.07.032>

- CUMMINGS.N.W. (1935). Evaporation from water surfaces: Status of present knowledge and need for further investigations, Transactions of the American Geophysical Union, Vol. 16, issue 2, pp. 507–510.
<https://doi.org/10.1029/TR017i002p00507>
- CUNDERLIK J., SIMONOVIC S.P. (2004). Calibration, Verification, and Sensitivity Analysis of the HEC-HMS Hydrologic Model, *Water Resources Research Report*, No 11. <https://ir.lib.uwo.ca/wrrr/11>
- DEB S. (2024). Optimizing hydrological exploration through GIS-based groundwater potential zoning in Gomati district, Tripura, India, Larhyss Journal, No 60, pp. 231-256.
- DERDOUR A., BOUANANI A., BABAHAMED K (2017). Floods typology in semiarid environment: case of Ain Sefra watershed (Ksour mountains, Saharian atlas, SW of Algeria), Larhyss Journal, No 29, pp. 283-299. (In French)
- DJELLOULI F., BOUANANI A., BABA-HAMED K. (2015). Hydrological characterization of the Oued Louza basin using a global rainfall-flow model, Larhyss Journal, No 23, pp. 275-286. (In French)
- DOUMOUNIA A., ZEBA A., DAMIBA L., ZOUGMORE F, NIKIEMA M. (2020). Climate variability analysis in the Nouhao sub-basin in eastern center of Burkina Faso, Larhyss Journal, No 41, pp. 57-69. (In French)
- EL HMAIDI A., LAYADI A., BOUFALA M., EL ABASSI M., ESSAHLAOUI A. (2015). Contribution of GIS in selecting the favorable site for the location of the station purifying wastewater of Azrou city (middle atlas, Morocco), Larhyss Journal, No 21, pp. 7-14.
- FAREGH W., BENKHALED A. (2016). GIS based SCS-CN method for estimating runoff in Sigus watershed, Larhyss Journal, No 27, pp. 257-276. (In French)
- FERESHTEHPOUR M., ESMAEILZADEH M., ALIPOUR R.S., BURIAN S.J. (2024). Impacts of Digital Elevation Model type and resolution on deep learning-based flood inundation mapping, *Earth Science Informatics*, Vol. 17, Issue 2, pp. 1125-1145.
<https://doi.org/10.1007/s12145-024-01239-0>
- FERNANDO H.M.S., GUNAWARDENA M.P., NAJIM M.M.M. (2021). Modelling of stream flows of a forested catchment in the tropics using HEC-HMS, Larhyss Journal, No 48, pp. 73-89.
- FLEMING S.W. (2009). An Informal Survey of Watershed Model Users: Preferences, Applications, and Rationales, *Streamline Watershed Management Bulletin*, Vol. 13, Issue 1, pp. 32-35.
- GASSI K.A.A., SAOUDI H. (2023). The effect of the physical parameterization schemes in WRF-ARW on the quality of the prediction of heavy rains that cause flooding application on eastern Algeria, Larhyss Journal, No 56, pp. 123-137.

- GOLIAN S., SAGHAFIAN B., ELMI M., MAKNOON R. (2011). Probabilistic rainfall thresholds for flood forecasting: evaluating different methodologies for modelling rainfall spatial correlation (or dependence), *Hydrological Processes*, Vol. 25, Issue 13, pp. 2046-2055. <https://doi.org/10.1002/hyp.7956>
- GOPINATH G., SWETHA T.V., ASHITHA M.K. (2014). Automated extraction of watershed boundary and drainage network from SRTM and comparison with Survey of India toposheet, *Arabian Journal of Geosciences*, Vol. 7, Issue 3, pp. 2625-2632. <https://doi.org/10.1007/s12517-013-0919-0>
- GUPTA H.V., SOROOSHIAN P.O. YAPO. (1999). Status of automatic calibration for hydrologic models: Comparison with multilevel expert calibration, *Journal Hydrological Engineering*, Vol. 4, Issue 2, pp. 135-143. [https://doi.org/10.1061/\(ASCE\)1084-0699\(1999\)4:2\(135\)](https://doi.org/10.1061/(ASCE)1084-0699(1999)4:2(135))
- HACHEMI A., BENKHALED A. (2016). Flood-duration-frequency modeling application to wadi Abiodh, Biskra (Algeria), *Larhyss Journal*, No 27, pp. 277-297.
- HAFNAOUI M.A., BOULTIF M., DABANLI I. (2023). Floods in Algeria: analyzes and statistics, *Larhyss Journal*, No 56, pp. 351-369.
- HAMIMED A., ZAAGANE M., OUALID A.T., TEFFAHI M., BAKHTIAR D. (2017). Monitoring daily actual evapotranspiration and surface water status over an agricultural area in western Algeria using remote sensing data, *Larhyss Journal*, No 29, pp. 45-59.
- HOUICHI L. (2017). Appropriate formula for estimating rainfall intensity of selected duration and frequency: a case study, *Larhyss Journal*, No 30, pp. 67-87. (In French)
- HOUNTONDJI B., CODO F.P., DAHOUNTO S.V.H., GBAGUIDI T.B. (2019). Flood management in urban environment: case of the Cotonou city in Benin, *Larhyss Journal*, No 39, pp. 333-347. (In French)
- JAFARZADEGAN K., MERWADE V. (2017). A DEM-based approach for large-scale floodplain mapping in ungauged watersheds, *Journal of Hydrology*, Vol. 550, Issue 2, pp. 650-662. <https://doi.org/10.1016/j.jhydrol.2017.04.053>
- JAISWAL T., JHARIYA D., SINGH S. (2023). Identification and mapping of groundwater potential zone using analytical hierarchy process and GIS in lower Kharun basin, Chhattisgarh, India, *Larhyss Journal*, No 53, pp. 117-143.
- JOO J., KJELDSSEN T., KIM H. J., LEE H. (2014). A comparison of two event-based flood models (ReFH-rainfall runoff model and HEC-HMS) at two Korean catchments, Bukil and Jeungpyeong, *KSCE Journal of Civil Engineering*, Vol. 18, Issue 1, pp. 330-343. <https://doi.org/10.1007/s12205-013-0348-3>
- KANG B., RAMÍREZ J.A. (2007). Response of streamflow to weather variability under climate change in the Colorado Rockies, *Journal of Hydrologic Engineering*, Vol. 12, Issue 1, pp. 63-72. [https://doi.org/10.1061/\(ASCE\)1084-0699\(2007\)12:1\(63\)](https://doi.org/10.1061/(ASCE)1084-0699(2007)12:1(63))

- KERBOUB D., CHAMEKH K., FEHDI C., BOUDOUKHA A.R. (2016). Contribution of G.I.S in mapping pollution, case of the El-Kantara plain, south east of Algeria, Larhyss Journal, No 27, pp. 175-185. (In French)
- KHERDE R.V., MEHTA D.J., MORE K.C., SAWANT P.H. (2024). Dynamic watershed modelling: HEC-HMS analysis of a tropical watershed, Larhyss Journal, No 60, pp. 87-111.
- KONETI S., SUNKARA S.L., ROY P.S. (2018). Hydrological modeling with respect to impact of land-use and land-cover change on the runoff dynamics in Godavari River Basin using the HEC-HMS model, International Society for Photogrammetry and Remote Sensing, International Journal of Geo-Information, Vol. 7, Issue 6, pp. 1-17. <https://doi.org/10.3390/ijgi7060206>
- KOUAO J.M., KOUASSI A.M., DEKOULA S.C., ASSEUFI B.D. (2020). Analysis of the climate regionalization of the ivory coast in a changing climate context, Larhyss Journal, No 41, pp. 233-259. (In French)
- KOUASSI A.M., KOUAME K.F., SALEY M.B., BIEMI J. (2013). Impacts of climate change on groundwater of crystalline and Crystallophyllian basement aquifers in west Africa: case of the N'zi-Bandama watershed (Ivory Coast), Larhyss Journal, No 16, pp. 121-138. (In French)
- KOUSSA M., BERHAIL S. (2021). Evaluation of spatial interpolation techniques for mapping groundwater nitrates concentrations - case study of Ain Elbel-sidi Makhoulouf syncline in the Djelfa region (Algeria), Larhyss Journal, No 45, pp. 119-140.
- KUMAR M.G., AGARWAL A.K., BALI R. (2008). Delineation of potential sites for water harvesting structures using remote sensing and GIS, Journal of the Indian Society of Remote Sensing, Vol. 36, Issue 4, pp. 323-334. <https://doi.org/10.1007/s12524-008-0033-z>
- LERAT J., PERRIN C., ANDRÉASSIAN V., LOUMAGNE C., RIBSTEIN P. (2012). Towards robust methods to couple lumped rainfall-runoff models and hydraulic models: A sensitivity analysis on the Illinois River, Journal of Hydrology, Vol. 418, Issue 2, pp. 123-135. <https://doi.org/10.1016/j.jhydrol.2009.09.019>
- MAH D.Y.S., DAYANG NUR HUWAIDA A.S., TEO F.Y. (2023). Investigation of historical extreme rainfall on permeable road in a commercial centre, Larhyss Journal, No 53, pp. 165-182.
- MAH D.Y.S., ALHADI H.F., BATENI N., TEO F.Y. (2024). Model simulation of dry stormwater detention pond with IPCC AR6 projected climate change scenarios, Larhyss Journal, No 60, pp. 151-169.
- MAITY R., RAMADAS M., GOVINDARAJU R.S. (2013). Identification of hydrologic drought triggers from hydroclimatic predictor variables, Water Resources Research, Vol. 49, Issue 7, pp. 4476-4492. <https://doi.org/10.1002/wrcr.20346>

- MEENU R., REHANA S., MUJUMDAR P.P. (2013). Assessment of hydrologic impacts of climate change in Tunga–Bhadra river basin, India with HEC-HMS and SDSM, *Hydrological processes*, Vol. 27, Issue 11, pp. 1572-1589.
<https://doi.org/10.1002/hyp.9220>
- MEHTA D., HADVANI J., KANTHARIYA D., SONAWALA P. (2023). Effect of land use land cover change on runoff characteristics using curve number: A GIS and remote sensing approach, *International Journal of Hydrology Science and Technology*, Vol. 16, Issue 1, pp. 1-16.
- MEHTA D., YADAV S. (2024). Rainfall runoff modelling using HEC-HMS model: case study of Purna river basin, *Larhyss Journal*, No 59, pp. 101-118.
- NAKOU T.R., SENOU L., ELEGBEDE B., CODO F.P. (2023). Climate variability and its impact on water resources in the lower mono river valley in Benin from 1960 to 2018, *Larhyss Journal*, No 56, pp. 215-234.
- NEZZAL F., BELKEBIR R., BENHAIDA A (2015). Risk of flooding in the watershed of the Oued Hamiz (Bay of Algiers), *Larhyss Journal*, No 22, pp. 81-89. (In French)
- N'GUESSAN BI V.H., ADJAKPA T.T., ALLECHY F.B., YOUAN TA M., ASSA Y.F. (2020). Characterization of the drought by the SPI and SPEI indices in the west center of Côte d'Ivoire case of the Lobo basin, *Larhyss Journal*, No 43, pp. 23-39.
- NICHANE M., KHELIL M.A. (2015). Climate change and water resources in Algeria - vulnerability, impact and adaptation strategy, *Larhyss Journal*, No 21, pp. 25-33. (In French)
- NIEHOFF D., FRITSCH U., BRONSTERT A. (2002). Land-use impacts on storm-runoff generation: scenarios of land-use change and simulation of hydrological response in a meso-scale catchment in SW-Germany, *Journal of hydrology*, Vol. 267, Issue 1-2, pp. 80-93. [https://doi.org/10.1016/S0022-1694\(02\)00142-7](https://doi.org/10.1016/S0022-1694(02)00142-7)
- PANDEY P., MISHRA R., CHAUHAN R.K. (2022). Future prospects in the implementation of a real-time smart water supply management and water quality monitoring system, *Larhyss Journal*, No 51, pp. 237-252.
- PANG J.M., TAN K.W. (2023). Development of regional climate model (RCM) for Cameron highlands based on representative concentration pathways (RCP) 4.5 and 8.5, *Larhyss Journal*, No 54, pp. 55-70.
- PAPATHANASIOU C., MAKROPOULOS C., MIMIKOU M. (2015). Hydrological modelling for flood forecasting: Calibrating the post-fire initial conditions, *Journal of Hydrology*, Vol. 529, Issue 3, pp. 1838-1850.
<https://doi.org/10.1016/j.jhydrol.2015.07.038>
- PATEL K., MEHTA D. (2022). Design of the continuous water supply system using Watergems software: a case study of Surat city, *Larhyss Journal*, No 50, pp. 125-136.

- QURESHI H.U., ABBAS I., SHAH S.M.H., TEO F.Y. (2024). Hydrologic evaluation of monthly and annual groundwater recharge dynamics for a sustainable groundwater resources management in Quetta city, Pakistan, *Larhyss Journal*, No 60, pp. 27-53.
- RANZI R., BOCHICCHIO M., BACCHI B. (2002). Effects on floods of recent afforestation and urbanisation in the Mella River (Italian Alps), *Hydrology and Earth System Sciences*, Vol. 6, Issue 2, pp. 239-254. <https://doi.org/10.5194/hess-6-239-2002>
- RAO A.R., HAMED K.H. (2001). *Flood Frequency analysis*. CRC Press, New York, USA.
- RAO K.H.V.D., RAO V.V., DADHWAL V.K., BEHERA G., SHARMA J.R. (2011). A distributed model for real-time flood forecasting in the Godavari Basin using space inputs, *International Journal of Disaster Risk Science*, Vol. 2, Issue 3, pp. 31-40. <https://doi.org/10.1007/s13753-011-0014-7>
- RAWAT.K. S., KRISHNA G., MISHRA A., SINGH J., MISHRA S.V. (2014). Effect of DEM data resolution on low relief region sub-watershed boundaries delineating using of SWAT model and DEM derived from CARTOSAT-1 (IRS-P5), SRTM and ASTER, *Journal of Applied and Natural Science*, Vol.6, Issue 1, pp. 144-151. <https://doi.org/10.31018/jans.v6i1.391>
- REMINI B. (2019). The Oasis of El Guerrara (Algeria): irrigation and recharge of the aquifers ensured by the floods, *Larhyss Journal*, No 40, pp. 135-163. (In French)
- REMINI B. (2020). Algeria: the climate is changing, the water is becoming scarce, what to do? *Larhyss Journal*, No 41, pp. 181-221. (In French)
- REMINI B. (2023). Flash floods in Algeria, *Larhyss Journal*, No 56, pp. 267-307.
- REMINI B. (2024). Dams in the face of climate change! *Larhyss Journal*, No 59, pp. 229-241.
- RICHARDSON B. (1931). Evaporation as a function of insolation, *Transactions of the American Society of Civil Engineers*, Vol. 95, Issue 1, pp. 996-1011. <https://doi.org/10.1061/TACEAT.0004284>
- ROY D., BEGAM S., GHOSH S., JANA S. (2013). Calibration and validation of HEC-HMS model for a river basin in Eastern India, *Asian Research Publishing Network Journal of Engineering and Applied Sciences*, Vol. 8, Issue 1, pp. 40-56.
- SAIDI S., AMMAR S., Jlassi F., BOURI S. (2016). Urban expansion and its impact on water resources using remote sensing and GIS: Case of great Tunis, *Larhyss Journal*, No 28, pp. 87-101. (In French)
- SAHU S., SUPE J., RATHORE K., VERMA S., MEHTA D. (2024). An integrated approach for evaluating water quality, *Larhyss Journal*, Vol. 60, pp. 213-230.

- SAMAKÉ Y., ASSEMIAN A.E., SORO N. (2021). Cartography of the zones favourable to the implantation of drilling center of the Côte d'Ivoire, *Larhyss Journal*, No 45, pp. 7-33.
- SAMANTA S., PAUL S.K. (2016). Geospatial analysis of shoreline and land use/land cover changes through remote sensing and GIS techniques, *Modeling Earth Systems and Environment*, Vol. 2, Issue 3, Paper ID 108.
<https://doi.org/10.1007/s40808-016-0180-0>
- SHARMA M.P. KUJUR A. (2012). Application of Remote Sensing and GIS for groundwater recharge zone in and around Gola Block, Ramgargh, *International Journal of Scientific and Research Publications*, Vol. 2, Issue 2, pp. 2–7.
- SHAIKH A.F., BHIRUD Y.L., MORE S.B., PAWAR A.D., VAIDYA O.V. (2024). Comparative analysis of optimization algorithms for reservoir operations: a case study on Ukai dam, *Larhyss Journal*, No 58, pp. 179-196.
- SINGH V.P., WOOLHISERD A. (2002). Mathematical Modeling of Watershed Hydrology, *Journal of Hydrologic Engineering*, Vol. 7, Issue 4, pp. 270-292.
[https://doi.org/10.1061/\(ASCE\)1084-0699\(2002\)7:4\(270\)](https://doi.org/10.1061/(ASCE)1084-0699(2002)7:4(270))
- SONI S., DEWANGAN C.L., AHMAD I., SARKAR H., VERMA V. (2023). Application of geospatial technique and hydrological modelling in evaluating reservoir sedimentation in Chhattisgarh state of India. *Indian Society for Hydraulics, Journal of Hydraulic Engineering*, Vol. 29, Issue 1, pp. 419-433.
<https://doi.org/10.1080/09715010.2023.2236985>
- SORO G.E., NOUFE D., GOULA BI T.A. (2018). Sensitivity analysis of a global hydrological model to the estimates of average rainfall and potential evapotranspiration: application to the Marahoue basin in Cote d'Ivoire, *Larhyss Journal*, No 23, pp. 115-168. (In French)
- TIBANGAYUKA N., MULUNGU D. M., IZDORI F. (2022). Evaluating the performance of HBV, HEC-HMS, and ANN models in simulating streamflow for a data scarce high-humid tropical catchment in Tanzania, *Hydrological Sciences Journal*, Vol. 67, Issue 14, pp. 2191-2204.
<https://doi.org/10.1080/02626667.2022.2137417>
- TRAMBLAY Y., BOUVIER C., AYRAL P.A., MARCHANDISE A. (2011). Impact of rainfall spatial distribution on rainfall-runoff modelling efficiency and initial soil moisture conditions estimation, *Natural Hazards and Earth System Sciences*, Vol. 11, Issue 1, pp. 157-170. <https://doi.org/10.5194/nhess-11-157-2011>
- TRIVEDI M., SURYANARAYANA T.M.V. (2023). An assessment of optimal operation policies for a reservoir using particle swarm optimization, *Larhyss Journal*, No 56, pp. 107-121.

- VALENCIA ORTIZ J.A., MARTÍNEZ-GRAÑA A.M. (2024). Evaluation of flood exposure in anthropic environments applied to different areas in the region of Bucaramanga, Colombia, *Geomatics, Natural Hazards and Risk*, Vol. 15, Issue 1, pp. 2375544. <https://doi.org/10.1080/19475705.2024.2375544>
- VAN CHINH L., ISERI H., HIRAMATSU K., HARADA M., MORI M. (2013). Simulation of rainfall runoff and pollutant load for Chikugo River basin in Japan using a GIS-based distributed parameter model, *Paddy and Water Environment*, Vol. 11, Issue 3, pp. 97-112. <https://doi.org/10.1007/s10333-011-0296-9>
- VERMA S., VERMA M.K., PRASAD A.D., MEHTA D.J., ISLAM M.N. (2024a). Modeling of uncertainty in the estimation of hydrograph components in conjunction with the SUFI-2 optimization algorithm by using multiple objective functions, *Modeling Earth Systems and Environment*, Vol. 10, Issue 1, pp. 61-79.
- VERMA S., SAHU R.T., PRASAD A.D., VERMA M.K. (2023). Reservoir operation optimization using ant colony optimization a case study of Mahanadi reservoir project complex Chhattisgarh – India, *Larhyss Journal*, No 53, pp. 73-93.
- VERMA S., PRASAD A.D. VERMA M.K. (2024b). Optimal operation of the multi-reservoir system: a comparative study of robust metaheuristic algorithms, *International Journal of Hydrology Science and Technology*, Vol. 17, Issue 3, pp.239-266. <https://doi.org/10.1504/IJHST.2024.137773>
- VERMA S., PRASAD A.D. VERMA M.K. (2024c). A framework for the evaluation of MRP complex precipitation in a CORDEX-SA regional climate applied to REMO, *International Journal of Hydrology Science and Technology*, Vol. 17, Issue 1, pp.17-45. <https://doi.org/10.1504/IJHST.2024.135125>
- VERMA S., PRASAD A.D., VERMA M.K. (2022c). Time series modelling and forecasting of mean annual rainfall over MRP Complex Region Chhattisgarh associated with climate variability, *Proceeding of Recent Advances in Sustainable Environment*, Vol. 285, pp. 51-67. https://doi.org/10.1007/978-981-19-5077-3_5
- VERMA S., SAHU R.T., PRASAD A.D. VERMA M.K. (2022b). Development of an optimal operating policy of multi-reservoir systems in Mahanadi Reservoir Project Complex, Chhattisgarh, *Journal of Physics: Conference Series*, Vol. 2273, Issue 1, pp. 1-13. [10.1088/1742-6596/2273/1/012020](https://doi.org/10.1088/1742-6596/2273/1/012020)
- VERMA S.K., SAHU R.T., SINGH H., PRASAD A.D., VERMA M.K. (2022a). A study of Environmental and Ecological impacts due to Construction and Operation of Tehri-Polavaram Dam, *Institute of Physics Conference Series: Earth and Environmental Science*, Vol. 1032, Issue 1, pp. 1-8. [10.1088/1755-1315/1032/1/012020](https://doi.org/10.1088/1755-1315/1032/1/012020)
- WARBURTON M.L., SCHULZE R.E., JEWITT G.P. (2012). Hydrological impacts of land use change in three diverse South African catchments, *Journal of Hydrology*, Vol. 414, Issue 1, pp. 118-135. <https://doi.org/10.1016/j.jhydrol.2011.10.028>

- YASIN Z., NABI G., RANDHAWA S.M. (2015). Modeling of hill torrent using HEC Geo-HMS and HEC-HMS models: A case study of Mithawan watershed, Pakistan Journal of Meteorology Vol, 11, Issue 22, pp. 1-11.
- YOUNG C.C., LIU W.C., CHUNG C.E. (2015). Genetic algorithm and fuzzy neural networks combined with the hydrological modeling system for forecasting watershed runoff discharge, Neural Computing and Applications, Vol. 26, Issue 7, pp. 1631-1643. <https://doi.org/10.1007/s00521-015-1832-0>
- YUKSEL A., GUNDOGAN R., AKAY A.E. (2008). Using the remote sensing and GIS technology for erosion risk mapping of Kartalkaya dam watershed in Kahramanmaras, Turkey, Sensors, Vol. 8, Issue 8, pp. 4851-4865. <https://doi.org/10.3390/s8084851>
- ZEGAIT R., REMINI B., BENSAHA H. (2021). Groundwater vulnerability assessment in the M'Zab valley - southern Algeria, Larhyss Journal, No 48, pp. 211-234.
- ZEGAIT R., PIZZO H.S. (2023). Flood control reservoir using VBA simulation case of Idles basin in southern Algeria, Larhyss Journal, No 53, pp. 41-60.
- ZHANG H.L., WANG Y.Q.J., WANG Y.Q.J., LI D.X., WANG X.K. (2013). The effect of watershed scale on HEC-HMS calibrated parameters: A case study in the Clear Creek watershed in Iowa, US, Hydrology and Earth System Sciences, Vol. 17, Issue 7, pp. 2735- 2745. <https://doi.org/10.5194/hess-17-2735-2013>.